On the adaptability of 1/1 cubic approximant structure in the Mg-Al-Zn system with the particular example of Mg$_{32}$Al$_{12}$Zn$_{37}$

Pierre Montagné, Monique Tillard

Agrégats, Interfaces, Matériaux pour l'Energie

Institut Charles Gerhardt, UMR-5253 CNRS, UM2, CC1502,

Université de Montpellier 2, Sciences et Techniques du Languedoc,

2 Place Eugène Bataillon, 34095 Montpellier Cedex, FRANCE

CORRESPONDING AUTHOR: Monique TILLARD

Email mtillard@univ-montp2.fr, phone 33 4 67 14 48 97, fax 33 4 67 14 33 04.

Abstract

Intermetallic Mg alloys are of interest in the development of light materials with specific properties and some of them are crystalline approximants of quasicrystalline materials. $Mg_{32}Al_{12}Zn_{37}$ single crystal structure, cubic, $Im\overline{3}$, a = 14.1845(1) Å, is disordered and belongs to the well known 1/1 approximant structural type commonly called $Mg_{32}(Al_{1-x}Zn_x)_{49}$ or T-phase. In this family, $Mg_{32}Al_{12}Zn_{37}$ is a new member remarkable for its very special composition nearby intersection of the 2/1 and 1/1 lines that mark composition domains of cubic 2/1 and 1/1 approximants. Structural features are discussed comparatively with literature data to emphasize the great adaptability through atom disorder of the 1/1 structure.

1. *Introduction*

The magnesium alloys are attractive for their special properties and have been of great interest in the development of light and high strength alloys to meet industrial or commercial requirements. Systems based on these elements have been thus investigated many times with the aim of understanding processes and better controlling the casting techniques. The discovery of quasicrystalline compounds in various Al-based systems has further motivated many studies, particularly explorations in the ternary Mg-Al-Zn system. The recently reported diagram [1] shows quite complex thermal equilibriums and two ternary phases are identified in this system. The first, labeled Φ, has been approximated to a stoichiometric compound of formula $Mg_5Al_2Zn_2$ or $Mg_6(Al_{1-x}Zn_x)_5$ [2-4]. Its composition domain is quite narrow with a limited Mg-content (53 to 55 at.%) but spreads over a wide range of Al/Zn ratio (0.64 - 1.7). The second phase, reported there as T-phase but elsewhere as R-phase [5], extends over a larger domain ranging from 32 to 42 at.% Mg, 13 to 49 at.% Al and 10 to 49 at.% Zn. Even though Mg-content is known to vary by a few percents, this phase is commonly reported as $Mg_{32}(Al_{1-x}Zn_x)_{49}$. As it was first identified by Bergmann [6], the term "Bergman line" has been used to designate its composition domain. At that time, this cubic structure was described by means of atom coordinations (12 to 16) and polyhedral duality. Further investigations established its relationship with icosahedral quasicrystals and shown that it should be considered as a crystalline approximant of type 1/1 [7]. Many stoichiometries are reported in the literature for Mg-Al-Zn alloys, of which some correspond to quasicrystalline materials [8]. In most cases, crystalline and quasicrystalline compounds are identified based on their powder diffraction patterns [9, 10], more rarely single crystal structures are provided [11, 12]. As evidenced, quasicrystals may form in this system over a wide range of compositions, those formed along the Bergman line are regarded as metastable while those, Mg-rich with low Al-contents (12-15 at.%) are found thermally more stable [13, 14]. Quasicrystals of the former class convert into crystals with the 1/1 structure type (T-phase) under heating at ~300 °C [9, 13, 14]. Instead members of the second class are stable up to ~450 °C and are located in the composition diagram near the 2/1-type domain along a line that we will call the 2/1 line. Cubic structure of type 2/1 was established for a few compositions but complete results are not always reported [15, 16]. Other Mg-rich crystalline compounds displaying the orthorhombic symmetry are reported as Φ-phase, the stability of which was studied together with its relationship with icosahedral quasicrystals [2-4].

This work brings reliable structural data for a disordered compound having a very special chemical composition. With a weak Al-content as 2/1 approximants, $Mg_{32}Al_{12}Zn_{37}$ however

belongs to the well known 1/1-type $Mg_{32}(Al_{1-x}Zn_x)_{49}$. It lies at one extreme of what has been reported before for T-phase, nearby intersection of 2/1 and 1/1 lines. Several structural features are discussed to emphasize the structural adaptability, unravel complexity of structures and contribute to better understanding of the ternary Mg-Al-Zn system.

2. *Experimental section*

Metal powders (Mg, 99.8%, 20-100 mesh; Al, 99.5%, 325 mesh; Zn, 99.9%,140-325 mesh, Alfa Aesar) kept and handled in Ar atmosphere were weighed in appropriate amounts (45:15:40), intimately mixed and inserted in a Ta tube weld-sealed under argon protected from oxidation in an Ar-filled sealed stainless steel jacket. Samples were heated to 800 °C for 16 h and submitted to a continuous rotation to ensure a good homogenization. A subsequent thermal treatment, based on that reported for 2/1 approximant [16] was applied: cooling to 360 °C at 10 °/h, keeping temperature for 100 h before quenching in cold water. A part of the grey and shiny product, seemingly homogeneous and well crystallized, was ground and sieved for powder X-ray diffraction (XRD) experiments. Several crystals were selected under a microscope inside the glove box and sealed in capillaries to be checked for crystallinity. They all displayed cubic symmetry (a = 14.2Å) and the best diffracting one was chosen for data collection on the Xcalibur CCD (Oxford Diffraction) four-circle diffractometer using MoKα radiation (table 1). EDX analyses were performed using an Oxford Instrument Environmental Scanning Electron Microscope, equipped with an X-Max large area SDD sensor that allows excellent sensitivity/precision/resolution. For several large pieces, noticeable variations in composition indicated that the final product was not obtained as a single phase. On the other hand, the Mg:Al:Zn compositions of several identified single crystals were found very close to 39.7:14.9:45.6, that of the single crystal used for data collection. XRD patterns were recorded on a Philips analytical X'pert diffractometer equipped with a Cu tube and a hybrid monochromator (parabolic multilayer mirror and two-crystal). Treatment using the Rietveld procedure included in program Jana2006 [17] confirmed the presence of at least two components. Geometry optimizations have been performed at the DFT level with program CASTEP [18, 19] using GGA-PW91 exchange correlation functionals [20], ultra-soft pseudo-potentials [21] and a density-mixing scheme. Kinetic energy cut-off was set at 340 eV and a Monkhorst-Pack grid of *k*-points was used for numerical integration in Brillouin zone [22].

3. *Results and discussion*

3.1. Structural characterization

The XRD pattern analysis with cubic T-phase leaves unindexed lines that correspond to the orthorhombic Φ-phase (Pbcm, a = 8.89, b = 16.94 and c = 19.29 Å). In a two-phase profile refinement, cell parameters satisfactorily converge to values that are consistent with those previously published for the two compounds. Nevertheless, presence of a third unidentified component in very small amount cannot be rejected (very weak non indexed lines).

Table 1. Crystal data and structure refinement [1] for $Mg_{32}Al_{12}Zn_{37}$

Refined formula	$Mg_{31.64}Al_{11.62}Zn_{36.74}$
Space group, Z	$Im\bar{3}$ (n° 204), 2
Cell dimensions (Å)	a = 14.1845(1)
Crystal size (mm), μ (mm^{-1})	0.14 x 0.15 x 0.16, 15.638
Theta range (°), completeness	3.52 to 31.78, 99.6%
Data collected / independent	29599 / 901 [R(int) = 0.0374]
Refined parameters	43
Final indices I>2sigma(I) (*all data*)	*R1* = 0.0205 (*0.0227*), *wR2* = 0.0456 (*0.0460*)
Largest diff. peak and hole (e.Å^{-3})	0.399 and -0.984

Single crystal data clearly indicated centrosymmetry and I-centering, they are indexed within a cubic $Im\bar{3}$ lattice of parameter a = 14.1845(1) Å. Absorption effects were corrected using the procedure included in CrysAlis software [23] and the final data set used for full-matrix least-squares refinements (SHELXL97 [24]) consisted of 901 (857 with I > 2σ(I)) unique reflections. Among the 7 positions provided by direct methods (SHELXS97 [25]), 4 were assigned to Mg and 3 to metal atoms. Refinement of the model with Al-filling at metal sites led to R1 of ~13%, instead R1 dropped to ~7% for Zn-filling. From here, considering Al/Zn mixing at these sites drastically improved agreement factors. Nevertheless the refined formula $Mg_{52}Al_{37}Zn_{71}$ (normalized to 32.5:23.1:44.4) was too far from composition of the single crystal (EDX). On the other hand, one site over the four initially assigned to Mg showed a displacement parameter significantly higher than others. Some reports state that this site 12e (x,0,½) is affected by a less common Mg/Zn disorder (elements differing from almost 10% in their Pauling radii) [11, 26] which was considered here. The position is found completely filled contrary to what is observed

for the $Mg_{2-y}(Al_{1-x}Zn_x)_{3+y}$ series with only ~60% filling [11, 26]. Note that refinements with similar atom distribution and 12e partial filling gave in this case unsatisfactory results, particularly regarding the compound composition. At remaining Mg sites, freely refined factors did not deviate, within standard limits, from the full site occupancy. It is worthy to mention that several studies considered the 2a position (0,0,0) either partially or even completely filled in isostructural compounds [6, 26-29].
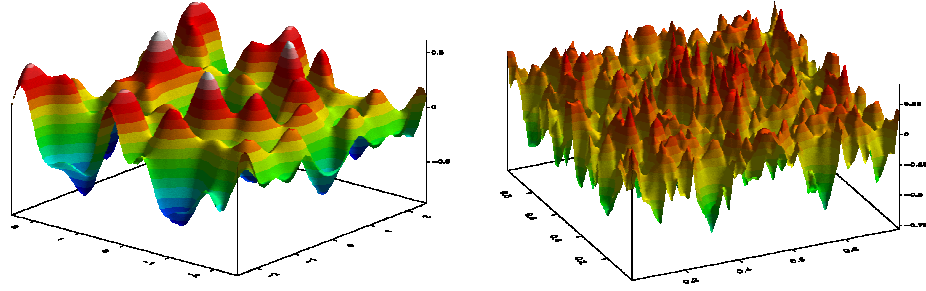

Fig. 1. Residual electron density maps around the 2a site. Highest peak and deepest hole, 0.4 and –0.9 e.Å^{-3}, are close to (0.09, 0.04, 0.13) and (0.0, 0.0, 0.03).

No residual electron density is observed in present structure (Fig. 1), excluding the presence of any atom at 2a, yet separated by 2.52Å from M1 at icosahedron vertices. This finding is consistent with results reported for isostructural compounds [11, 12] in MgAlZn or in other systems, as for instance Li_3CuAl_5 and $Li_{13}Cu_6Ga_{21}$ [30, 31].

Table 2. Atom coordinates ($\times 10^4$) and displacement parameters (Å$^2 \times 10^3$) in $Mg_{32}Al_{12}Zn_{37}$. U_{eq} is defined as one third of the trace of the orthogonalized U_{ij} tensor.

	label	site	occupancy	x	y	z	U_{eq}
Zn/Al(1)	M1	24g	0.873/0.127(6)	0	929(1)	1512(1)	10(1)
Zn/Al(2)	M2	24g	0.722/0.278(6)	0	1803(1)	3066(1)	13(1)
Zn/Al(3)	M3	48h	0.719/0.281(5)	1574(1)	1916(1)	4035(1)	13(1)
Mg(1)/Zn(4)	M4	12e	0.941/0.059(4)	4023(1)	0	5000	16(1)
Mg(2)	A1	12e		1981(1)	0	5000	17(1)
Mg(3)	A2	16f		1861(1)	1861(1)	1861(1)	15(1)
Mg(4)	A3	24g		0	3006(1)	1163(1)	15(1)

Positions and anisotropic displacement parameters were refined for all atoms, together with ratios Al/Zn at M1-M3 and Mg/Zn at M4, to R1 = 2.05% (table 2). Unit cell content converged to 63.29 Mg, 23.24 Al and 73.47 Zn, that is a ratio Mg:Al:Zn of 39.6:14.5:45.9 which agrees quite well

with analysis of the single crystal (39.7:14.9:45.6). Compound can be formulated $Mg_{31.64}Al_{11.62}Zn_{36.74}$ with Z = 2 as well as $Mg_{2-y}(Al_{1-x}Zn_x)_{3+y}$ with x = 0.76, y = 0.022 and Z = 32. In the following, the rounded formula $Mg_{32}Al_{12}Zn_{37}$ (or $Mg_{32}(Al_{1-x}Zn_x)_{49}$ for x = 0.76) will be used to refer to this compound.

3.2. Structural description and discussion

$Mg_{32}Al_{12}Zn_{37}$, cubic, $Im\overline{3}$, a = 14.1845(1) Å, Z = 2 represents a new chemical composition for the already known structure $Mg_{32}(Al_{1-x}Zn_x)_{49}$ or T-phase. Its close-packed structure is dominated by icosahedral concentric shells around the 2a empty site. Polyhedra occur in the characteristic sequence of Bergman cluster: M_{12} icosahedron, A_{20} pentagonal dodecahedron, M_{12} icosahedron and M_{60} Samson polyhedron. The icosahedral 5-fold symmetry could extend within this 104-atom cluster $Al_{1.5}Zn_{10.5}@Mg_{20}@Al_{3.3}Zn_{8.7}@Mg_{11.3}Al_{13.5}Zn_{35.2}$ (Fig. 2). Al and Zn are mixed at both innermost (M1) and larger (M2) icosahedra, respectively at 2.52 and 5.05 Å from 2a center. Between the two, the dodecahedral shell (8×A2+12×A3) at 4.57 Å is only formed by Mg. From 6.68 to 7.26 Å, on the outer M_{60} shell (12×M4+48×M3), Zn is partially replaced by Mg at M4 and by Al at M3 sites. Consequently, Mg/Zn (M4-M4) edges are somewhat lengthened, 2.77 Å, compared to Al/Zn (M3-M3) edges of 2.67 Å.
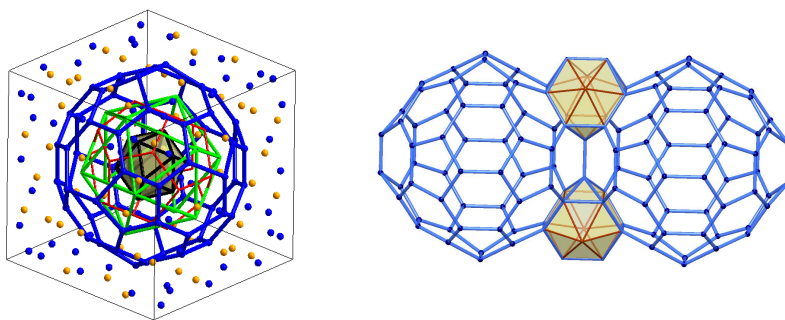

Fig. 2. The Bergman endohedral cluster $Al_{1.5}Zn_{10.5}@Mg_{20}@Al_{3.3}Zn_{8.7}@Mg_{11.3}Al_{13.5}Zn_{35.2}$ and polyhedral packing in $Mg_{32}Al_{12}Zn_{37}$

The M_{60} units join by sharing M4-M4 hexagon-edge (Fig. 2) and interstitial space is filled by wedge-shaped polyhedra $Mg@Mg_{2.8}Al_{2.3}Zn_{5.9}$ (around A1) that allow packing of M_{60} units within a periodic 3-dimensional arrangement. These polyhedra are thus essential elements in formation of crystalline rather than quasicrystalline arrangements. It is at M_{60} shell and at a less extent at junction polyhedra which one observes the largest atom mixing phenomena that involves three atom species. This is quite a common feature for crystalline approximants of type 1/1 and

$Mg_{32}Al_{12}Zn_{37}$, with an electron to atom ratio e/a of 2.14, conforms to this general trend. However one must mention that perfectly ordered Bergman's polyhedra also exist, as for example the unit $Ga_{12}@Li_{20}@Cu_{12}@Ga_{60}$ at 2a empty center in isostructural $Li_{13}Cu_6Ga_{21}$ (e/a = 2.05) [31]. On the contrary, M_{60} shell is strongly affected by atom disorder and sometimes additionally by occupation disorder in MgAlZn compounds. Samson's surface is the place where major disorder phenomena are observed, it is also the place where the failure in propagation of the 5-fold symmetry necessarily happens. This is a zone of important strain where frustrations must be relaxed through distortions or deviations from perfect 5-fold symmetry to allow the packing of polyhedral units (close to icosahedral symmetry) within a cubic 3-D periodic arrangement. Atom deviations from the ideal positions [7], here 0.03-0.07Å except 0.2 Å for M4, give a measure of this distortion. Stabilization into a crystalline network may depend upon atom distribution in this boundary region. Such an interpretation is supported by the theoretical analysis of hypothetical models $Mg_{32}Al_{49}$ [11] which states that vacancy formation and atomic Al/Zn adjustment are crucial in tuning the VECs (valence electron counts or e/a) and in reducing antibonding interactions. This can be illustrated with the Zn-content at each metal site plotted in Fig. 3 vs. the total Zn-content, for $Mg_{32}Al_{12}Zn_{37}$ and isostructural compounds [11, 12]. At first sight, Zn proportion at M1 to M3 displays an overall trend to increase with the total Zn-content but things are not as neat for M4.
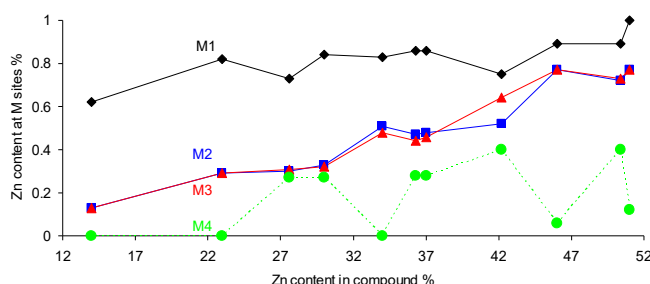

Fig. 3. Zn-content at M sites for Mg-Al-Zn T-phases containing 14 to 51 at.% of Zn.

The M1 site on the internal icosahedron is mainly filled by Zn, in proportions limited between 62-100 at.%. On larger icosahedral and M_{60} shells, Zn-contents at M2 and M3 are curiously very similar over the whole composition range and regularly increase from 13 to 77 at.%. It becomes clear that these sites will be important in the structure capability to absorb the Al/Zn compositional variations. In most cases M4 site is entirely filled and Zn-free but examples are known where Zn is present in well defined proportions (27 or 40%) at this non-fully filled Mg site therefore complemented by vacancies [11]. This suggests that Mg for Zn substitution process would occur by steps. In $Mg_{32}Al_{12}Zn_{37}$ (or $Mg_{39.6}Al_{14.5}Zn_{45.9}$), the M4 entire filling is achieved

with a low but non-zero Zn-content of 6 at.% (*i.e.* 11.3 Mg and 0.7 Zn) tending to invalidate such an assumption. It should be noticed that a rather similar situation, with 10.6 Mg and 1.4 Zn, is reported for the Zn-rich compound $Mg_{39.5}Al_{9.2}Zn_{51.5}$ [12]. Such analysis of the distribution of atoms different in nature over the various sites is a helpful tool to better understand the great adaptability of the 1/1 cubic structure. Thus, sites M3 and M4 on M_{60} shell, take a significant part in phenomena that lead to accommodate the structural arrangement with different atomic and/or electronic contents.

3.3. Structural preferences

Compound $Mg_{32}Al_{12}Zn_{37}$, the object of this work, is remarkable by its particular chemical composition, with both a weak Al-content as in approximants of type 2/1 and a weak Mg-content as in approximants of type 1/1, the two well-known structures for crystalline cubic arrangements in relation to quasicrystals. Let us compare stoichiometry $Mg_{32}Al_{12}Zn_{37}$ with $Mg_{46}Al_{17}Zn_{37}$ [16], that of a 2/1 approximant ($Pa\overline{3}$, a ~23.1 Å). Even though they have close Al/Zn ratios, they significantly differ in their Mg-content. Based on a general review of literature reports, it is obvious that Mg-richest compounds adopt the 2/1 structure type. Instead, type 1/1 is favored for low Mg-contents. To better visualize their respective domains, we have reported in a composition diagram a series of compounds quoted in literature (Fig. 4). Crystalline approximant materials of types 1/1 or 2/1 are represented as circles and triangles while quasicrystalline materials are marked as rhombuses. The 1/1 line, also called Bergman line, represents the existence domain of the 1/1 structure type (T-phase, $Im\overline{3}$, a ~14.2 Å) and the 2/1 line delimits the region where occurs the 2/1 structure type ($Pa\overline{3}$, a ~23.1 Å). Note worthy are the positions distributed along these lines over a large composition domain, of various stoichiometries of materials identified as quasicrystals. The orthorhombic Φ-phase (square marks) is observed for Mg-rich compositions (~55 at.%) and Zn-contents from 20 to 40 at.%. In other words, one can consider the Φ-phase to mainly occur along a parallel with the 1/1 line. This structure is adopted by several compounds which can be formulated $Mg_{55-\varepsilon}(Al_{1-x}Zn_x)_{45+\varepsilon}$, x ranging from 0.44 to 0.89 [2-4]. The metastable phase Mg_4AlZn_{11} known as η' phase [32] which is of little interest in the current context (far from the focused region) is not reported in the diagram. Looking at Fig. 4, it is clear that all phases that display the 2/1 structure have very similar Al-contents (close to 15 at.%) but variable Mg/Zn proportions. The Zn-content therein ranges from 14 to 56 at.%, thus 2/1 approximants can be formulated as $Al_{15-\varepsilon}(Mg_{1-x}Zn_x)_{85+\varepsilon}$ with $0.16 \leq x \leq 0.66$.
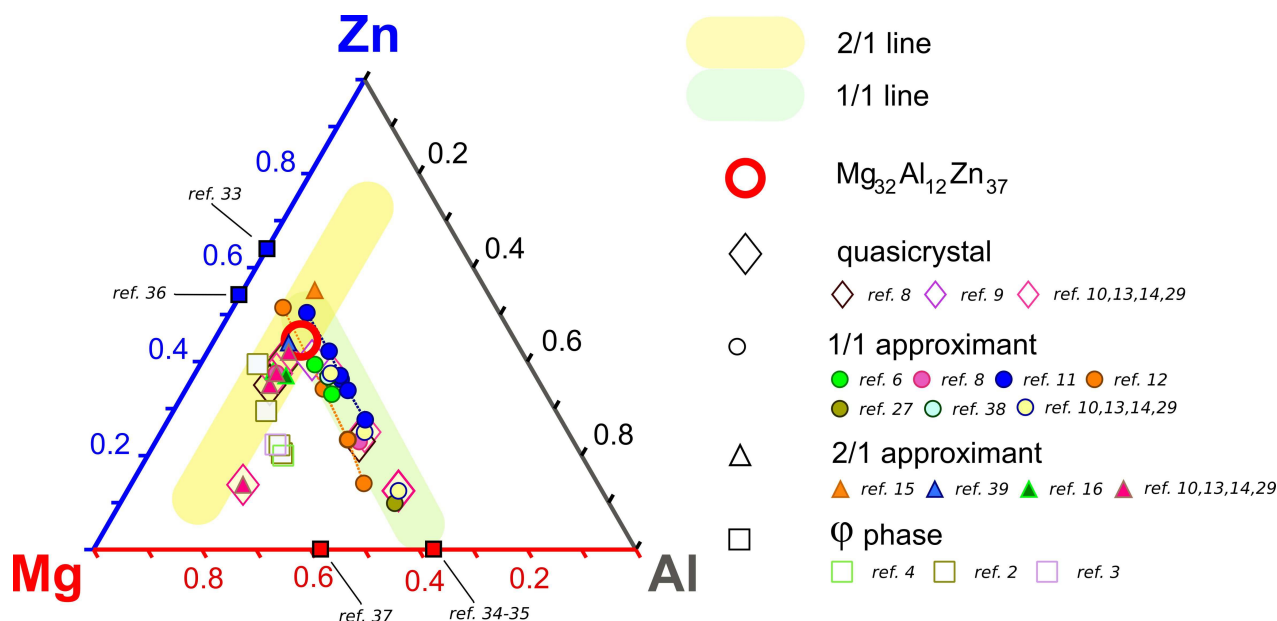
Fig. 4. Composition diagram reporting various compounds characterized and identified in literature. Circle: T-phase (cubic 1/1 approximant); triangle: cubic 2/1 approximant, rhombus: quasicrystalline materials, square: orthorhombic Φ-phase.

With close Mg-contents and Al/Zn variable proportions, the 1/1 structure type has many representatives in an extremely large composition domain [6, 9, 12, 27]. It is commonly called $Mg_{32}(Al_{1-x}Zn_x)_{49}$ for $0.16 \leq x \leq 0.85$, but it is also appropriate to designate this family using the normalized equivalent formula $Mg_{39}(Al_{1-x}Zn_x)_{61}$ in which Zn-content ranges from 9.8 to 51.5 at.%. Compound $Mg_{32}Al_{12}Zn_{37}$, otherwise formulated $Mg_{39}Al_{15}Zn_{46}$, is one of the Zn-richest compounds displaying this structural type. Its position in the diagram, marked with a large red circle, is particularly interesting since it lies at intersection of the 1/1 and 2/1 lines associated with corresponding structural types. As a consequence of its very particular position it can be formulated $Mg_{39}(Al_{1-x}Zn_x)_{61}$, x = 0.754 or $Al_{15}(Mg_{1-x}Zn_x)_{85}$, x = 0.541, and one can expect for $Mg_{32}Al_{12}Zn_{37}$ an ability to crystallize within the two structural types.

Let us return now to the experimental conditions of synthesis. $Mg_{32}Al_{12}Zn_{37}$ was obtained from Mg:Al:Zn in proportions 45:15:40, a stoichiometry taking place on the 2/1 line just between lines associated with T-phase (type 1/1) and Φ-phase. Note the complexity in this region where some imprecision remain [2] and where stoichiometries could correspond to crystalline approximants 1/1 or 2/1, to quasicrystalline materials and even to crystalline Φ-phase (also in relation with icosahedral quasicrystals [4]). Therefore it is easy to understand that experimental conditions will play a decisive part in the formation of compounds. What could seem an obvious assertion takes a huge importance here, in a case where very subtle changes can have a major impact on both

composition and structure of the final alloy. In this chemical composition domain, a given combination might yield each of the structural types mentioned above. Moreover, crystalline and quasicrystalline materials with almost identical stoichiometries can coexist. One could simply state that a kind of competition exists between the various structures and that extremely small variations in experimental conditions will favor either one or the other atomic/structural arrangement. Under these conditions, reproducing an experiment becomes a quite difficult task. This is well illustrated by the different kinds of marks -triangles, circles, rhombuses- observed in a very limited composition domain (Fig. 4). It is then likely that the prepared alloy contains a small amount of 2/1 crystalline or even of quasicrystalline phases, which would explain the weak lines remaining unindexed in XRD pattern refined with T-phase as major component and Φ-phase as side product. This is also in agreement with the possibility to formulate $Mg_{32}Al_{12}Zn_{37}$ ($Mg_{39}Al_{15}Zn_{46}$) both using the 1/1 or 2/1 approximants general formula. If present in the alloy, a quasicrystalline component can belong to one or the other kind of quasicrystals.

Only four binary phases selected for their singular positions are reported in the diagram (Fig. 4). Except for Mg_2Al_3, they are described with totally ordered atomic arrangements. The Bergman line would be extended to Mg_4Zn_7 (or $Mg_{36}Zn_{64}$) [33] and Mg_2Al_3 (or $Mg_{37.3}Al_{62.7}$, according to its true formula [34, 35]). Similarly, $Mg_{21}Zn_{25}$ (or $Mg_{45.7}Zn_{54.3}$, e/a = 2) [36] and $Mg_{17}Al_{12}$ (or $Mg_{58.6}Al_{41.4}$, e/a = 2.41) [37] are located at both ends the Φ-phase domain. Moving along the Bergman line from Mg_4Zn_7 to Mg_2Al_3, the e/a ratio increases from 2 to 2.66. Between these limits the T-phases are characterized by values in range 2.09-2.49, close to the e/a ratios of 2.18 and 2.55 given for the $Mg_{2-y}(Al_{1-x}Zn_x)_{3+y}$ phase width [11]. On the other hand, the 2/1 structural type is observed in a narrow domain from 2.12 to 2.20, just as the Φ-phase from 2.10 to 2.25. In spite of such special positions, no structural relationship can be established as for instance a structural change with the progressive substitution of Zn for Al along the concentration range. Despite a metric relationship in lattice dimensions (doubled parameter), Mg_2Al_3 cannot be considered as a boundary of the T-phase domain even though its composition, in fact $Mg_{37.3}Al_{62.7}$, does not deviate much from the general formula $Mg_{39}(Al_{1-x}Zn_x)_{61}$ and perfectly fits the alternate formula $Mg_{2-y}(Al_{1-x}Zn_x)_{3+y}$ for y = 0.13. Actually, $Mg_{37.3}Al_{62.7}$ is characterized by a high level of positional and atomic disorder and it can be assumed that occurrence of such a disorder is the result of packing frustrations and electronic constraints (too high e/a of 2.66) that prevent and make unrealizable the atom arrangement in the T-phase structure type. Subsequently the adaptability of the 1/1 structure is apparently restricted, with variable atom composition and consequently electron concentration, to a domain which does not expand to the most distant binary compositions. Within its whole composition domain the T-phase would be considered as a solid

solution, then its lattice parameter is expected to vary with Al/Zn ratio according to Vegard's law. Cell parameter of $Mg_{32}Al_{12}Zn_{37}$ fairly well agrees with the available data for a series of compounds characterized with a filled M4 position (circles, Fig. 5) [12]. With M4 partial filling, $Mg_{2-y}(Al_{1-x}Zn_x)_{3+y}$ have slightly lower parameters (triangles, X-ray and rhombuses, neutron) suggesting that a lower Mg-content could be accountable for a cell contraction.
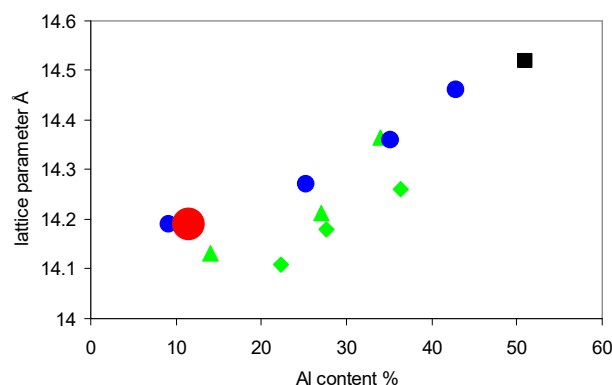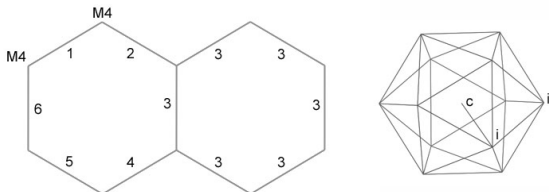

Fig. 5. Lattice parameter vs. Al-content in T-phases. Large red circle: $Mg_{32}Al_{12}Zn_{37}$, blue circles [12], green triangles and rhombuses [11], black square [27].

With the intention to provide supplemental elements to the structural analysis, DFT calculations were carried out for ordered models established starting from the experimental structure of $Mg_{32}Al_{12}Zn_{37}$. Accurate geometries were optimized within cubic symmetry and unit cell dimensions did not deviate from the experimental by more than 3.5%. Since Mg predominates at M4, an Mg atom was placed at this position and then filling Al/Zn sites either with Al or Zn led to the models $Mg_{32}Al_{48}$ and $Mg_{32}Zn_{48}$. From here, models $Mg_{26}Al_{54}$ and $Mg_{26}Zn_{54}$ were built with Al or Zn at M4 and models $Mg_{32}Al_{49}$ and $Mg_{32}Zn_{49}$ with Al or Zn additional centering at site 2a. The optimized cells are significantly smaller for Zn models and volumes both increase with Mg-content and with icosahedron centering (table 3). Such behavior is in good agreement with experimental findings, i.e. parameter is reduced when Mg-content decreases or when Al- or Zn-content increases. The formation enthalpy, defined as the difference in total energies calculated for compound and for elements in their solid state structures, is a useful tool to evaluate relative stabilities. Negative values of about -50 and -170 meV/atom (table 3) indicate that compounds may form with such stoichiometries. Because of small differences in energy, stabilization effects would be quite weak. Nevertheless, the slightly higher enthalpies computed for models $Mg_{32}M_{49}$ offer some support for non-centering of the Bergmann unit. The transformation of $Mg_{32}M_{48}$ into $Mg_{26}M_{54}$ (by Mg replacement at M4) leads to opposite effects in Al and Zn models, respectively destabilized by 7 or stabilized by 10 meV/atom. This would account for the numerous variants of

ternary compounds reported with this structural type because stability would be reached for a balance between stoichiometry and atom distribution. Therefore a compromise has to be found between various parameters to fulfill stability and structural requirements.

Table 3. Optimized lattice parameter (Å), distances (Å) and formation enthalpy (meV/atom)

	1	2	3	4	5	6	c-i	i-i	a	ΔHf
$Mg_{26}Al_{54}$	2.70	3.01	2.76	2.76	2.77	3.01	2.61	2.74	14.5130	-0.048
$Mg_{32}Al_{48}$	2.87	3.03	2.75	2.81	2.75	3.03	2.62	2.74	14.6195	-0.055
$Mg_{32}Al_{49}$	2.89	3.05	2.76	2.82	2.76	3.05	2.70	2.82	14.6835	-0.045
$Mg_{26}Zn_{54}$	2.49	2.94	2.66	2.79	2.66	2.94	2.47	2.59	13.9262	-0.174
$Mg_{32}Zn_{48}$	2.76	2.92	2.64	2.77	2.64	2.92	2.49	2.61	14.0848	-0.164
$Mg_{32}Zn_{49}$	2.78	2.93	2.65	2.78	2.65	2.93	2.61	2.72	14.1304	-0.162
$Mg_{32}Al_{12}Zn_{37}$	2.77	2.94	2.67	2.73	2.67	2.94	2.52	2.64	14.1845	

Deformation charge density computed by subtracting densities of isolated atoms from the total electron density is mapped at M_{60} surface for models $Mg_{32}M_{48}$ and $Mg_{26}M_{54}$ (Fig. 6). As it represents the electron redistribution due to chemical bonding, it is very informative on the nature of interactions. Highest positive values are associated with bond formation and lowest negative values point out electron losses. A glance at these maps clearly shows changes in the electron redistribution with the nature of atoms. This is particularly well illustrated at specific M4-M4 pair with clearly non bonding interactions for Mg ($Mg_{32}M_{48}$), bonding for Zn ($Mg_{26}Zn_{54}$) and strongly bonding for Al ($Mg_{26}Al_{54}$). Optimized distances (table 3) indicate a significant enlargement of the central icosahedron but no effects on the M_{60} shell for 2a-filling. On the contrary, changing nature of atoms at M4 not only affects distances but also create distortion, as exemplified in $Mg_{26}Zn_{54}$ with the hexagon which clearly deviates from flatness. This provides a graphic illustration of the constraints mentioned above that occur at this shell where atomic and electronic adjustments take place.
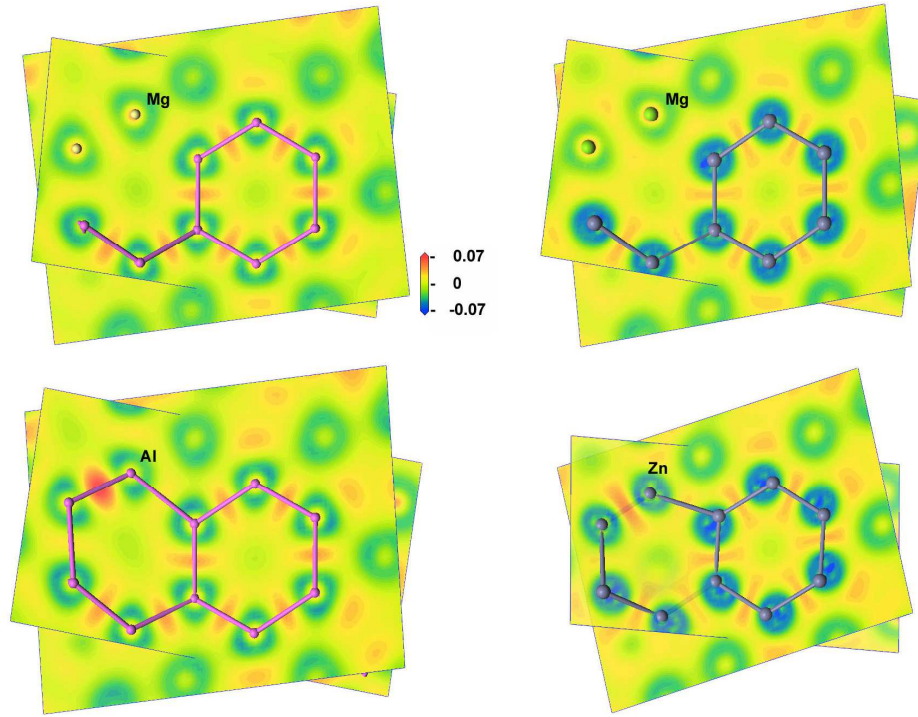
Fig. 6. CASTEP electron density difference at M_{60} shell showing a clearly non bonding character at Mg pairs in $Mg_{32}Al_{48}$ (up left) and $Mg_{32}Zn_{48}$ (up right) and bond formation (red zones) at Al and Zn pairs in $Mg_{26}Al_{54}$ (down left) and $Mg_{26}Zn_{54}$ (down right)

4. Conclusion

$Mg_{32}Al_{12}Zn_{37}$ prepared and characterized displays a special composition. With a weak Al-content, it could be described with both generic formula of 1/1 and 2/1 crystalline approximant, but its belongs to the 1/1 structure type well known as $Mg_{32}(Al_{1-x}Zn_x)_{49}$. A comparative analysis with regard to a series of compositions taken from the literature highlights the complexity of this ternary system, particularly in an area where subtle changes in experimental conditions could favor one or the other crystalline or even quasicrystalline forms. The structural study brings a proof of vacuity at the cell origin in $Mg_{32}Al_{12}Zn_{37}$, a result supported by DFT calculations. Atom disorder is not evenly distributed on the whole structure, innermost shells mainly consist of Mg and disorder preferentially occurs at outer shells. This is reflected by the formula $Al_{1.5}Zn_{10.5}@Mg_{20}@$ $Al_{3.3}Zn_{8.7}@Mg_{11.3}Al_{13.5}Zn_{35.2}$ of the endohedral 104-atom cluster. The diversity of arrangements on the M_{60} shell, sometimes including vacancy defects, accounts for the great adaptability of the structure which is able to accommodate variable atomic and electronic compositions.

References

[1] V. Raghavan, *J. Phase Equilib. Diffus.*, 28 (**2007**) 203-208.

[2] R. Berthold, G. Kreiner, U. Burkhardt, S. Hoffmann, G. Auffermann, Y. Prots, E. Dashjav, A. Amarsanaa, M. Mihalkovic, *Intermetallics*, 32 (**2013**) 259-273.

[3] L. Bourgeois, B.C. Muddle, J.F. Nie, *Acta Mater. *, 49 (**2001**) 2701-2711.

[4] A. Singh, J.M. Rosalie, H. Somekawa, T. Mukai, *J. Alloys Comp.*, 509 (**2011**) 4676-4681.

[5] H.K. Hardy, J.M. Silcock, *J. Inst. Met. *, 24 (**1955**) 423.

[6] G. Bergman, J.L.T. Waugh, L. Pauling, *Acta Crystallogr.*, 10 (**1957**) 254-259; *Nature* 1069 **(1952)** *1057-1058.*

[7] C.L. Henley, V. Elser, *Philos. Mag. B*, 53 (**1986**) L59-L66.

[8] A. Matsumuro, J. Fujita, K. Kato, *J. Mater. Sci. Lett. *, 16 (**1997**) 2032-2035.

[9] T. Rajasekharan, D. Akhtar, R. Gopalan, K. Muraleedharan, *Nature*, 322 (**1986**) 528-530.

[10] T. Takeuchi, U. Mizutani, *Phys. Rev. B*, 52 (**1995**) 9300-9309.

[11] C.-S. Lee, G.J. Miller, *J. Am. Chem. Soc.*, 122 (**2000**) 4937-4947.

[12] W. Sun, F.J. Lincoln, K. Sugiyama, K. Hiraga, *Mater. Sci. Eng., A*, 294 (**2000**) 327-330.

[13] U. Mizutani, T. Takeuchi, T. Fukunaga, *Mater. Trans. *, 34 (**1993**) 102-108.

[14] T. Takeuchi, S. Murasaki, A. Matsumuro, U. Mizutani, *J. Non-Cryst. Solids*, 156-158, Part 2 (**1993**) 914-917.

[15] Q. Lin, J.D. Corbett, *PNAS*, 103 (**2006**) 13589-13594.

[16] K. Sugiyama, W. Sun, K. Hiraga, *J. Alloys Comp.*, 342 (**2002**) 139-142.

[17] V. Petricek, M. Dusek, L. Palatinus, *Z. Kristallogr.*, 229(5) (**2014**) 345-352.

[18] G. Kresse, J. Forthmuller, *J. Comput. Mater. Sci.*, 6 (**1996**) 15.

[19] G. Kresse, J. Forthmuller, *Phys. Rev. B* 54 (**1996**) 11169.

[20] J.P. Perdew, J.A. Chevary, S.H. Vosko, M.R. Pederson, D.J. Singh, C. Fiolhais, *Phys. Rev. B*, 46 (**1992**) 6671.

[21] D. Vanderbilt, *Phys. Rev. B*, 41 (**1990**) 7892-7895.

[22] H.J. Monkhorst, J.D. Pack, *Phys. Rev. B*, 16 (**1997**) 1748.

[23] CrysAlis'Red' 171 software package, Oxford diffraction Ltd, Abingdon, United Kingdom.

[24] G.M. Sheldrick, (**1997**) SHELXL97: A Program for Refining Crystal Structures. University of Göttingen. Germany.

[25] G.M. Sheldrick, (**1997**) SHELXS 97. A Program for Crystal Structures Solution. University of Göttingen. Germany.

[26] C.-S. Lee, G.J. Miller, *Inorg. Chem.*, 40 (**2001**) 338-345.

[27] J.H. Auld, B.E. Williams, *Acta Crystallogr. *, 21 (**1966**) 830-831

[28] G. Kreiner, S. Spiekermann, *J. Alloys Comp.*, 261 (**1997**) 62-82.

[29] U. Mizutani, W. Iwakami, T. Takeuchi, M. Sakata, M. Takata, *Philos. Mag. Lett*, 5 (**1997**) 34

[30] M. Audier, J. Pannetier, M. Leblanc, C. Janot, J.-M. Lang, B. Dubost, *Physica B: Condensed Matter*, 153 (**1988**) 136-142.

[31] M. Tillard-Charbonnel, C. Belin, *J. Solid State Chem.*, 90 (**1991**) 270-278.

[32] J.H. Auld, S.M. Cousland, *J. Austr. Inst. Met.*, 19 (**1974**) 194-199.

[33] Y.P. Yarmolyuk, P.I. Krypyakevych, E.V. Mel'nik, *Sov. Phys. Crystallogr. (Engl. Transl.)* 20 (**1975**) 329-331.

[34] M. Feuerbacher, C. Thomas, J.P.A. Makongo, S. Hoffmann, W. Carrillo-Cabrera, R. Cardoso, Y. Grin, G. Kreiner, J.-M. Joubert, T. Schenk, J. Gastaldi, H. Nguyen-Thi, N. Mangelinck-Noël, B. Billia, P. Donnadieu, A. Czyrska-Filemonowicz, A. Zielinska-Lipiec, B. Dubiel, T. Weber, P. Schaub, G. Krauss, V. Gramlich, J. Christensen, S. Lidin, D. Fredrickson, M. Mihalkovic, W. Sikora, J. Malinowski, S. Brühne, T. Proffen, W. Assmus, M. de Boissieu, F. Bley, J.-L. Chemin, J. Schreuer, W. Steurer, *Z. Kristallogr.*, 222 (**2007**) 259–288.

[35] P. Montagné, M. Tillard, *J. Solid state Electrochem.*, 19 (**2015**) 685-695.

[36] R. Cerny, G. Renaudin, *Acta Crystallogr. C*, 58 (**2002**) i154-i155.

[37] P. Schobinger Papamantellos, P. Fischer, *Naturwiss.*, 57 (**1970**) 128-129

[38] K. Riederer, *Z. Metallkd.*, 28 (**1936**) 312-317.

[39] S. Spiekermann, G. Kreiner (**1998**) *ISIS Experimental report*, cited in ref 15. www.isis.rl.ac.uk/ISIS98/reports/9566.pdf.